Proceedings of the American Control Conference
Arlington, VA June 25-27, 2001

Emergency Braking Control with an Observer-based Dynamic Tire/road Friction Model and Wheel Angular Velocity Information*

Jingang Yi†, Luis Alvarez‡, Xavier Claeys§, Roberto Horowitz¶ and Carlos Canudas de Wit‖

†,¶ *Department of Mechanical Engineering, University of California, Berkeley, CA 94720-1740, USA*
‡ *Instituto de Ingeniería Universidad Nacional Autónoma de México, 04510 Coyoacán DF, México*
§,‖ *Laboratoire d'Automatique de Grenoble, UMR CNRS 5528, ENSIEG-INPG, ST. Martin d'Hŕes, France*

Abstract

A control scheme for emergency braking of vehicles is designed. The scheme utilizes a LuGre dynamic friction model to estimate the tire/road friction. The control system output is the pressure to the braking system, and is calculated using only the wheel angular speed information. The controller utilizes estimated state feedback control to achieve near maximum deceleration. The state observer gain is calculated by using linear matrix inequality (LMI) techniques. This system has two advantages when compared with an antilock braking system (ABS), it generates less chattering during braking and produces a source of a priori information regarding safe spacing.

1 Introduction

In recent years, a significant amount of research has focused on investigating traffic safety in both manual traffic and Automated Highway Systems (AHS) when highway densities are significantly increased. One important issue that requires more analysis is the influence of the tire/road interaction on the braking capabilities of the vehicle and, therefore, on the overall highway safety. From the perspective of emergency braking, there are two main factors that influence the braking capacity of vehicle: tire/road friction and available braking torque. Both are difficult to determine precisely due to modeling complexities and variations in the operating conditions.

There is a significant amount of research in tire/road friction modeling and estimation for individual vehicles. The model given in [3], known as the "magic formula", gives a good approximation to quasi-static experimental results and is widely used in automotive research and industries. However, this model lacks a physical interpretation, has many parameters and these parameters are generally difficult to calibrate and identify. In [9] and [1] identifiable pseudo-static parametric friction models are presented. The parameters in these models lack a physical interpretation, but can be identified through on-line adaptations. A very nice property of the model given in [1] is the under-estimation of the friction coefficient and maximum slip ratio under normal driving conditions, which guarantees vehicle safety.

In recent years, dynamic friction models, such as the one presented in [5], have been proposed to capture the friction mechanism. These models have been used successfully to identify and compensate the friction in mechanical systems. In [6] a first-order friction dynamic model, called the *LuGre* model, was first introduced to replicate the tire/road interface. This model was used in [4] to estimate the tire/road friction coefficient under different road conditions, and applied in an adaptive braking controller in [11]. The calibration of its parameters and a comparison with the "magic formula" is also discussed in [11].

The goal of this paper is to extend the approach of [11]. In [11] the authors assume that all state variables are accessible. Here we relax this assumption by utilizing of a model-based observer, using only the angular velocity measurement of the wheel. A linear matrix inequality (LMI) technique is used to calculate the observer gains. The paper is divided into six sections. Section 2 describes the system dynamics. A compensator, which combines an adaptive controller with an observer, is presented in section 3. Simulation work is presented in section 4 and a discussion of the simulation results is given in section 5. Finally, section 6 contains concluding remarks and directions for future work.

2 System Dynamics

In this paper only the longitudinal dynamics of the vehicle is considered. We assume that the four wheels of the vehicle apply the same braking force. For simplicity, we also assume that the road has no slope and that the weight of the vehicle is distributed evenly among the four wheels. A quarter vehicle model is used and we consider

*Research supported by UCB-ITS PATH grant MOU-373 and a gift from Renault SA.

†Graduate student; Email: jgyi@me.berkeley.edu.
‡Professor; Email: alvar@pumas.iingen.unam.mx.
§Graduate student; Email: claeys@lag.ensieg.inpg.fr.
¶Professor and corresponding author; Email: horowitz@me.berkeley.edu.
‖Professor; canudas@lag.ensieg.inpg.fr.

a modified lumped LuGre friction model as follows:

$$\begin{cases} \dot{z} = -v_r - \theta \frac{\sigma_0 |v_r|}{h(v_r)} z \\ J\dot{\omega} = -rF_x - u_T \\ m\dot{v} = 4F_x - F_r \end{cases} \tag{1}$$

where z is the friction internal state, $v_r = v - r\omega$ is the relative velocity, $h(v_r) = \mu_c + (\mu_s - \mu_c)e^{-|\frac{v_r}{v_s}|^{1/2}}$, μ_s is the normalized static friction coefficient, μ_c is the normalized Coulomb friction, v_s is the Stribeck relative velocity, u_T is the traction/braking torque, F_x the traction/braking force given by the tire/road contacting, F_r the rolling resistance, m the vehicle mass, J the tire rotational inertia, and the parameter θ is used to model the effect of different tire/road Coulomb friction coefficients. The braking force F_x is given by

$$F_x = F_n(\sigma_0 z + \sigma_1 \dot{z} - \sigma_2 v_r)$$

where σ_0 is the rubber longitudinal stiffness, σ_1 is the rubber longitudinal damping, σ_2 is the viscous relative damping. F_x is a negative number in the case of braking and $F_n = mg/4$. By [10], the rolling resistance can be modeled as

$$F_r = \sigma_v mgv$$

where σ_v is rolling resistance coefficient and g is the gravity constant.

Defining the state variables as

$$x_1 := \sigma_0 z, \quad x_2 := v, \quad , x_3 := v_r = v - r\omega$$

the system dynamics Eq.(1) are rewritten as:

$$\dot{x}_1 = \sigma_0 \dot{z} = -\sigma_0 x_3 - \theta\sigma_0 f(x_3)x_1 \tag{2}$$

where $f(x_3) = \frac{x_3}{h(x_3)}$, here we use the fact that $x_3 = v_r = v - r\omega \geq 0$ during braking and

$$\dot{x}_2 = g\left[x_1 + \sigma_1(-x_3 - \theta f(x_3)x_1) - \sigma_2 x_3\right] - g\sigma_v x_2 \tag{3}$$

For the state variable x_3 we have

$$\begin{aligned} \dot{x}_3 = \dot{v} - r\dot{\omega} \quad &= \quad \alpha\left[x_1 + \sigma_1(-x_3 - \theta f(x_3)x_1) - \sigma_2 x_3\right] \\ &\quad -g\sigma_v x_2 + \frac{r}{J}K_b P_b, \end{aligned} \tag{4}$$

where $\alpha = g(1 + \frac{mr^2}{4J})$. In the above equation we use the formula $u_T = K_b P_b$, where K_b is the braking system gain and P_b the brake pressure, which is the controlled variable.

For most vehicles, we can measure the angular velocity of each wheel.

$$y = \omega = \frac{1}{r}(x_2 - x_3) \tag{5}$$

3 Observer-based Braking Controller Design

In this section we formulate the design of a controller based on the available angular velocity output. Arrange the system dynamics (2), (3), (4) and output measurements (5) as

$$\begin{cases} \dot{\mathbf{x}} = A\mathbf{x} + B_1\theta\psi(\mathbf{x}) + B_2 u \\ y = C\mathbf{x} \end{cases} \tag{6}$$

where

$$\mathbf{x} = \begin{bmatrix} x_1 \\ x_2 \\ x_3 \end{bmatrix}, \; A = \begin{bmatrix} 0 & 0 & -\sigma_0 \\ g & -g\sigma_v & -g(\sigma_2 + \sigma_1) \\ \alpha & -g\sigma_v & -\alpha(\sigma_2 + \sigma_1) \end{bmatrix},$$

$$B_1 = \begin{bmatrix} -\sigma_0 \\ -g\sigma_1 \\ -\alpha\sigma_1 \end{bmatrix}, \; B_2 = \begin{bmatrix} 0 \\ 0 \\ \frac{r}{J}K_b \end{bmatrix}, C = \begin{bmatrix} 0 & \frac{1}{r} & -\frac{1}{r} \end{bmatrix},$$

$$\psi(\mathbf{x}) = x_1 f(x_3), \quad u = P_b$$

Since the internal state z, given by the LuGre model, and the vehicle longitudinal velocity are unavailable, we must design an observer to estimate these states. We do so by constructing the following model-based nonlinear observer

$$\dot{\hat{\mathbf{x}}} = A\hat{\mathbf{x}} + B_1\hat{\theta}\psi(\hat{\mathbf{x}}) + B_2 u + L(y - C\hat{\mathbf{x}}) + B_1\mathcal{G} \tag{7}$$

where $\mathcal{G}$ is a tuning function to be determined subsequently.

The following assumptions are made for the system (6) and observer (7):

(i) (A, C) is a observable pair;

(ii) $f(x_3)$ is positive and bounded and $f'(x_3)$ is bounded, i.e.

$$\begin{aligned} 0 \leq f(x_3) \leq f_{max} \leq \rho_2 < \infty, \\ |f'(x_3)| \leq \rho_3 < \infty, \; \forall \mathbf{x} \in \mathcal{D}_1 \subset \mathcal{R} \end{aligned} \tag{8}$$

(iii) The unknown parameter θ is bounded, i.e.

$$0 < \theta \leq \theta_{max} \tag{9}$$

(iv) The map $w \mapsto \xi$ of the system

$$\begin{cases} \dot{\zeta} = (A - LC)\zeta + B_1 w \\ \xi = C\zeta \end{cases} \tag{10}$$

with $(A - LC)$ Hurwitz, is strictly passive; moreover, $\exists \rho_1 > 0$ a constant, and $\exists P = P^T > 0$ such that

$$(A - LC)^T P + P(A - LC) + (\rho_1^2 + \rho_4)I < 0 \tag{11}$$

as well as

$$PB_1 = C^T \tag{12}$$

where $\rho_4 = \frac{2\theta_{max}\rho_2}{r} > 0$.

Theorem 1 *Under assumptions (i) - (iv) there exists an adaptive emergency braking controller that achieves*

$$\hat{\lambda} \to \hat{\lambda}_{max}$$

asymptotically for the system (6) using measured angular velocity ω, where the estimated slip is given by $\hat{\lambda} := \frac{\hat{x}_3}{\hat{x}_2} = \frac{\hat{v}-r\hat{\omega}}{\hat{v}}$ and $\hat{\lambda}_{max} := \hat{\lambda}_{max}(\hat{v}_r, \hat{v})$ is the longitudinal slip corresponding to the estimated maximum friction coefficient $\hat{\mu}_{max}$ in the pseudo-static relationship between μ and λ.

Proof: Define $\tilde{\mathbf{x}} := \mathbf{x} - \hat{\mathbf{x}}$, $\tilde{y} := y - \hat{y} = C\tilde{\mathbf{x}}$ and $\tilde{\theta} := \theta - \hat{\theta}$, then the error dynamics for the system is

$$\dot{\tilde{\mathbf{x}}} = (A - LC)\tilde{\mathbf{x}} + B_1\left[\theta\psi(\mathbf{x}) - \hat{\theta}\psi(\hat{\mathbf{x}})\right] - B_1\mathcal{G} \quad (13)$$

define the dynamic surface $\tilde{s}$ as

$$\tilde{s} := \hat{x}_3 - \hat{\lambda}_{max}\hat{x}_2$$

differentiate $\tilde{s}$

$$\begin{aligned}
\dot{\tilde{s}} &= \dot{\hat{x}}_3 - \dot{\hat{x}}_2\hat{\lambda}_{max} - \dot{\hat{\lambda}}_{max}\hat{x}_2 \\
&= \frac{r}{J}K_bP_b - \sigma_1(\alpha - g\hat{\lambda}_{max})f(\hat{x}_3)\hat{\theta} + \\
&\quad \Big\{(\alpha - g\hat{\lambda}_{max})\left[\hat{x}_1 - (\sigma_2 + \sigma_1)\hat{x}_3 - \right. \\
&\quad \left.(1 - \hat{\lambda}_{max})g\sigma_v\hat{x}_2\right] + (l_3 - l_2\hat{\lambda}_{max})\tilde{y}\Big\} - \\
&\quad \sigma_1(\alpha - g\hat{\lambda}_{max})\mathcal{G} - \dot{\hat{\lambda}}_{max}\hat{x}_2 \\
&= dK_bP_b + \beta_1(\hat{\mathbf{x}})\hat{\theta} + \beta_2(\hat{\mathbf{x}}) + \beta_3(\hat{\mathbf{x}})\mathcal{G} \qquad (14)
\end{aligned}$$

where

$$d = \frac{r}{J}, \quad \beta_1(\hat{\mathbf{x}}) = -\sigma_1(\alpha - g\hat{\lambda}_{max})f(\hat{x}_3)\hat{x}_1,$$
$$\beta_2(\hat{\mathbf{x}}) = (\alpha - g\hat{\lambda}_{max})\left[\hat{x}_1 - (\sigma_2 + \sigma_1)\hat{x}_3\right] +$$
$$(l_3 - l_2\hat{\lambda}_{max})\tilde{y} - \dot{\hat{\lambda}}_{max}\hat{x}_2 - (1 - \hat{\lambda}_{max})g\sigma_v\hat{x}_2,$$
$$\beta_3(\hat{\mathbf{x}}) = -\sigma_1(\alpha - g\hat{\lambda}_{max}),$$

and l_2, l_3 are the second and third elements of the gain vector $L \in \mathcal{R}^3$.

Consider the following Lyapunov function candidate

$$V = \frac{1}{2}\tilde{s}^2 + \frac{1}{2\gamma}\tilde{\theta}^2 + \tilde{\mathbf{x}}^TP\tilde{\mathbf{x}}$$

where $\gamma > 0$. Then

$$\begin{aligned}
\dot{V} &= \dot{\tilde{\mathbf{x}}}^TP\tilde{\mathbf{x}} + \tilde{\mathbf{x}}^TP\dot{\tilde{\mathbf{x}}} + \tilde{s}\dot{\tilde{s}} + \frac{1}{\gamma}\tilde{\theta}\dot{\tilde{\theta}} \\
&= \tilde{\mathbf{x}}^T\left[(A - LC)^TP + P(A - LC)\right]\tilde{\mathbf{x}} + \\
&\quad 2\tilde{\mathbf{x}}^TPB_1\left[\theta\psi(\mathbf{x}) - \hat{\theta}\psi(\hat{\mathbf{x}})\right] + \frac{1}{\gamma}\tilde{\theta}\dot{\tilde{\theta}} + \tilde{s}\dot{\tilde{s}} - \\
&\quad 2\tilde{\mathbf{x}}^TPB_1\mathcal{G}
\end{aligned}$$

Notice that

$$\theta\psi(\mathbf{x}) - \hat{\theta}\psi(\hat{\mathbf{x}}) = \tilde{\theta}\psi(\hat{\mathbf{x}}) + \theta\left[\psi(\mathbf{x}) - \psi(\hat{\mathbf{x}})\right]$$

and use the assumption (12) to obtain

$$\begin{aligned}
\dot{V} &= \tilde{\mathbf{x}}^T\left[(A - LC)^TP + P(A - LC)\right]\tilde{\mathbf{x}} + \\
&\quad 2\tilde{y}\tilde{\theta}\psi(\hat{\mathbf{x}}) + 2\tilde{\mathbf{x}}^TPB_1\theta\left[\psi(\mathbf{x}) - \psi(\hat{\mathbf{x}})\right] + \\
&\quad \frac{1}{\gamma}\tilde{\theta}\dot{\tilde{\theta}} + \tilde{s}\Big[dK_bP_b + \beta_1(\hat{\mathbf{x}})\hat{\theta} + \beta_2(\hat{\mathbf{x}}) + \\
&\quad \beta_3(\hat{\mathbf{x}})\mathcal{G}\Big] - 2\tilde{\mathbf{x}}^TPB_1\mathcal{G}. \qquad (15)
\end{aligned}$$

Letting the control input be

$$u = P_b = \frac{1}{dK_b}\left[-\beta_1(\hat{\mathbf{x}})\hat{\theta} - \beta_2(\hat{\mathbf{x}}) - \beta_3(\hat{\mathbf{x}})\mathcal{G} - \eta\tilde{s}\right]$$

Eq.(14) becomes

$$\dot{\tilde{s}} = -\eta\tilde{s}. \qquad (16)$$

Using (12) and (16) and letting

$$\dot{\hat{\theta}} = 2\gamma\tilde{y}\psi(\hat{\mathbf{x}}) \qquad (17)$$

we obtain from Eq.(15)

$$\begin{aligned}
\dot{V} &= \tilde{\mathbf{x}}^T\left[(A - LC)^TP + P(A - LC)\right]\tilde{\mathbf{x}} + \\
&\quad 2\tilde{y}\tilde{\theta}\psi(\hat{\mathbf{x}}) + 2\tilde{\mathbf{x}}^TPB_1\theta\left[\psi(\mathbf{x}) - \psi(\hat{\mathbf{x}})\right] + \\
&\quad \frac{1}{\gamma}\tilde{\theta}\dot{\tilde{\theta}} - \eta\tilde{s}^2 - 2\tilde{y}\mathcal{G}.
\end{aligned}$$

Note that

$$\begin{aligned}
\psi(\mathbf{x}) - \psi(\hat{\mathbf{x}}) &= x_1f(x_3) - \hat{x}_1f(\hat{x}_3) \\
&= f(x_3)\tilde{x}_1 + \hat{x}_1f'(x_3^*)(x_3 - \hat{x}_3)
\end{aligned}$$

where x_3^* is a value between x_3 and $\hat{x}_3$ derived by using the Mean Value Theorem for the smooth function $f(x) = \frac{x}{h(x)}$. Moreover, by (8), (9) and (17)

$$
\begin{aligned}
\dot{V} &\leq \tilde{\mathbf{x}}^T\left[(A-LC)^TP+P(A-LC)\right]\tilde{\mathbf{x}} + \\
&\quad 2\tilde{\mathbf{x}}^TC^T\theta_{max}\rho_2\tilde{x}_1 + 2\rho_3\theta_{max}|\tilde{y}||\hat{x}_1||\tilde{x}_3| - \\
&\quad \eta\tilde{s}^2 - 2\tilde{y}\mathcal{G} \\
&= \tilde{\mathbf{x}}^T\left[(A-LC)^TP+P(A-LC)\right]\tilde{\mathbf{x}} + \\
&\quad \frac{1}{r}\theta_{max}\rho_2(2\tilde{x}_1\tilde{x}_2+2\tilde{x}_1\tilde{x}_3) + \\
&\quad 2\rho_3\theta_{max}|\tilde{y}||\hat{x}_1||\tilde{x}_3| - \eta\tilde{s}^2 - 2\tilde{y}\mathcal{G} \\
&\leq \tilde{\mathbf{x}}^T\left[(A-LC)^TP+P(A-LC)\right]\tilde{\mathbf{x}} + \\
&\quad \rho_4\left(\tilde{x}_1^2+\frac{1}{2}\tilde{x}_2^2+\frac{1}{2}\tilde{x}_3^2\right) - \frac{\rho_4}{2}\left(|\tilde{x}_3| - \frac{\rho_3 r}{\rho_2}|\tilde{y}\hat{x}_1|\right)^2 \\
&\quad +\frac{\rho_4}{2}\tilde{x}_3^2 + \frac{\rho_4}{2}\left(\frac{\rho_3 r}{\rho_2}\right)^2\hat{x}_1^2\tilde{y}^2 - \eta\tilde{s}^2 - 2\tilde{y}\mathcal{G} \\
&\leq \tilde{\mathbf{x}}^T\left[(A-LC)^TP+P(A-LC)+\rho_4 I\right]\tilde{\mathbf{x}} - \\
&\quad \eta\tilde{s}^2 - \frac{\rho_4}{2}\left(|\tilde{x}_3| - \frac{\rho_3 r}{\rho_2}|\tilde{y}\hat{x}_1|\right)^2 + \\
&\quad \tilde{y}\left[\frac{\rho_4}{2}\left(\frac{\rho_3 r}{\rho_2}\right)^2\hat{x}_1^2\tilde{y} - 2\mathcal{G}\right] \\
&\leq -\rho_1^2\|\tilde{\mathbf{x}}\|^2 - \eta\tilde{s}^2 - \frac{\rho_4}{2}\left(|\tilde{x}_3| - \frac{\rho_3 r}{\rho_2}|\tilde{y}\hat{x}_1|\right)^2 + \\
&\quad \tilde{y}\left[\frac{\rho_4}{2}\left(\frac{\rho_3 r}{\rho_2}\right)^2\hat{x}_1^2\tilde{y} - 2\mathcal{G}\right].
\end{aligned}
$$

If we choose $\mathcal{G}$ such that

$$
\mathcal{G} = \frac{\rho_4}{4}\left(\frac{\rho_3 r}{\rho_2}\right)^2\hat{x}_1^2\tilde{y} \tag{18}
$$

then

$$
\dot{V} \leq -\rho_1^2\|\tilde{\mathbf{x}}\|^2 - \eta\tilde{s}^2 - \frac{\rho_4}{2}\left(|\tilde{x}_3| - \frac{\rho_3 r}{\rho_2}|\tilde{y}\hat{x}_1|\right)^2 \leq 0
$$

using Barbalat's Lemma, we can conclude that

$$
\tilde{s} \to 0, \quad \tilde{\mathbf{x}} \to 0, \qquad \text{as } t \to \infty.
$$

Thus, by definition of $\tilde{s}$ and λ we have

$$
\hat{\lambda} \to \hat{\lambda}_{max} \qquad \text{as } t \to \infty
$$

■

Remark 1 The adaptive nonlinear observer structure presented in this paper is similar to the scheme presented in [7]. [7] presented results that require an additional Lipschitz assumption on the function $\psi(x)$, and condition (12) has been replaced by $B_1^TPC^{\perp} = 0$ where $C^{\perp}$ is the projection on to null(C).

Remark 2 The tuning function $\mathcal{G}$ given by (18) is a linear function of $\tilde{y}$ and appears both in the observer and the control input. Compared with the tuning function in [4], Eq. (18) does not require switching in the control input, and therefore produces a smoother control.

Remark 3 Assumptions (i) through (iv) must be satisfied in order for the system dynamics described by Eq. (6) and, thus for the theorem to hold:

(i) Regarding assumption (i), we can calculate the observability matrix of the system as follows,

$$
\mathcal{O} = \begin{bmatrix} 0 & \frac{1}{r} & -\frac{1}{r} \\ \frac{g-\alpha}{r} & 0 & \frac{a}{r} \\ \frac{\alpha a}{r} & -\frac{g\sigma_v a}{r} & \frac{(g-\alpha)\left[\alpha(\sigma_2+\sigma_1)^2+\sigma_0\right]}{r} \end{bmatrix}
$$

where $a = (\sigma_2+\sigma_1)(\alpha - g)$, thus $rank(\mathcal{O}) = 3$, and (A,C) is an observable pair. Hence, assumption (i) always holds;

(ii) To see that assumption (ii) is always satisfied, we have

$$
0 \leq f(x_3) = \frac{x_3}{h(x_3)} \leq \frac{x_3}{\mu_c} \leq \frac{\lambda_{max}v_{max}}{\mu_c} = \rho_2
$$

and

$$
|f'(x_3)| \leq \frac{1}{\mu_c}\left\{1 + \left(\frac{\mu_s}{\mu_c} - 1\right)\left[1 + \frac{1}{2}\left(\frac{v_{max}}{v_s}\right)^{1/2}\right]\right\} = \rho_3
$$

(iii) As for assumption (iv), we have to pick an observer gain L and a positive symmetric matrix P such that following optimization problem is feasible

$$
\begin{cases} \max & \rho_1 \\ \text{s.t.:} & (A-LC)^TP + P(A-LC) + \rho_1^2 I + \rho_4 I < 0 \\ & PB_1 = C^T, \quad P = P^T > 0 \text{ and } \rho_1 > 0 \end{cases}
$$

This can be calculated by linear matrix inequality (LMI) algorithms, such as those presented in [8].

4 Simulation Results

In the following simulation example we use the parameters from the LeSabre cars used by the California PATH program. These parameters are: $M = 1701.0\ Kg$, $Ca = 0.3693\ N\cdot s^2/m^2$, $J = 2.603\ Kg\cdot m^2$, $R = 0.323m$. We also take the road LuGre friction parameter in Eq.(1) parameter to be $\theta = 1$ and the braking gain $K_b = 0.9$. The nominal values of the parameters in the dynamic LuGre friction model are the same as those in [11].

We simulate an emergency braking maneuver with a vehicle initial velocity of $v = 30m/s$ and the designed observed-based controller. The initial condition for observer dynamics is $\hat{\mathbf{x}}(0) = [0\ 29.5\ 0]^T$ and the true state is $\mathbf{x}(0) = [0\ 30\ 0.5]^T$, namely we use the measurement $R\omega$ (=29.5m/s) as the initial condition for $\hat{v}$. Fig. 1 shows the time responses of the real state vector $\mathbf{x}$ and estimated state vector $\hat{\mathbf{x}}$, while Fig. 2(c) shows the time responses of the estimated friction parameter $\hat{\theta}$. Fig. 2(a) shows the time responses of the controlled

pressure P while Fig. 2(b) shows the controlled sliding surface $\tilde{s}$. Fig. 2(d) illustrates the difference, $\tilde{y}$, of measurement y and output of observer $\hat{y}$. From these figures we can see that the estimated state $\hat{z}$ and parameter $\hat{\theta}$ converge to their respective true values quickly, and that the controlled input (pressure P) remains within its feasible domain, enabling the vehicle to come to a quick halt (decelerating at around $10\,m/s^2$). This example verifies the results of the previous section. However, the simulation results also reveal that the estimated states $\hat{v}$ and $\hat{v}_r$ do not converge to their true states during the braking process, even though the vehicle achieved its maximum estimated deceleration level, which is based on estimated states, as shown by Fig. 2(b). We will discuss these results in more detail in the following section.

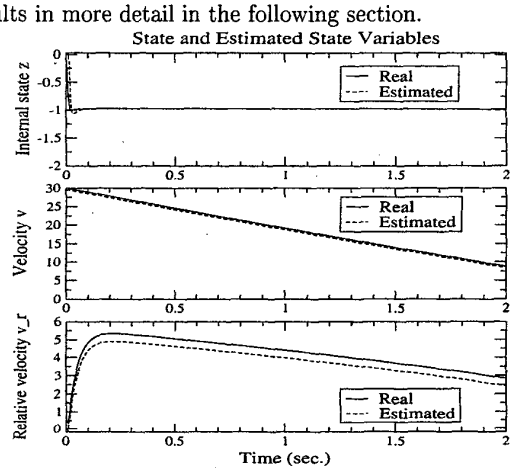

Figure 1: Estimated and real state variables.

5 Discussions

In the previous section we presented a simulation example in which the vehicle achieves its maximum estimated deceleration level in spite of the slow convergence rate of the control systems's estimated linear velocity error $\tilde{v}$ and relative velocity error $\tilde{v}_r$. In this section we produce an approximate analytical explanation of this result.

From the state error dynamics (13) we find

$$\dot{\tilde{y}} = -\frac{1}{r}[l_2 - l_3 + \sigma_1(g-\alpha)\mathbf{g}]\tilde{y} + f_1(\tilde{\mathbf{x}}) \qquad (19)$$

where $f_1(\tilde{\mathbf{x}}) = (g-\alpha)[(1-\sigma_1\theta f(x_3)]\tilde{x}_1 - \sigma_v\tilde{x}_2 - (\sigma_1 + \sigma_2)\tilde{x}_3 - \sigma_1[\theta f(x_3) - \hat{\theta} f(\hat{x}_3)]\hat{x}_1$ and $\mathbf{g} = \frac{\rho_4}{4}\left(\frac{\rho_3 r}{\rho_2}\right)^2 \hat{x}_1^2$. In our example, we chose a relative large value for the gain L with $l_2 > l_3$ ($L = [-400 \; -60 \; -500]^T$). As a consequence, $\tilde{y} \to 0$ quickly. Similarly, we can also assume that $\tilde{\theta} \to 0$ quickly due to our choice of a high adaptation gain $\gamma\,(= 200)$ and the presence of persistence of excitation, which we observed in the numerical example. A more thorough analysis to determine conditions for the existance of persistence of excitation is in progress.

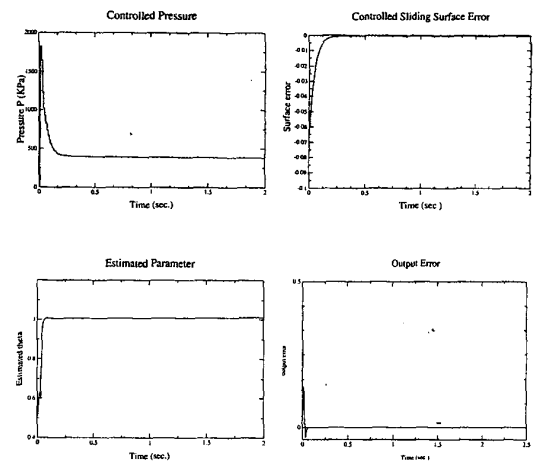

Figure 2: (a) Controlled braking pressure P and (b) sliding surface $\tilde{s}$ (c) Estimated friction parameter $\hat{\theta}$ and (d) measurement error $\tilde{y}$ (rad/s).

Using the approximation $\tilde{y} \approx 0$ and $\tilde{\theta} \approx 0$, we now analyze the dynamics of the state errors (13) and obtain

$$\dot{\tilde{\mathbf{x}}} = \bar{A}(x_3)\tilde{\mathbf{x}} \qquad (20)$$

where

$$\bar{A}(x_3) = \begin{bmatrix} -\sigma_0\theta f(x_3) & 0 & 0 \\ g[1-\sigma_1\theta f(x_3)] & -g\sigma_v & -g\sigma_2 \\ \alpha[1-\sigma_1\theta f(x_3)] & -g\sigma_v & -\alpha\sigma_2 \end{bmatrix}$$

Notice that $\sigma_0 = 280$, $\hat{\theta} \approx 1$ and $\frac{v}{\mu_c} \geq f(x_3) > \frac{v_r}{\mu_s}$. We can therefore conclude that $\tilde{x}_1 \to 0$ quickly with a decaying rate of around $\sigma_0\theta f(x_3)$ during the beginning of braking process, due to the fact that v_r is large. This explains why the estimated state $\hat{x}_1$ converges quickly to the real state x_1. In the case of the state estimates $\hat{x}_2$ and $\hat{x}_3$, from Eq.(20) we find that the eigenvalues of matrix $\bar{A}(x_3)$ associated with these two states are

$$s_{2,3} = \frac{-(g\sigma_v + \alpha\sigma_2) \pm \sqrt{(g\sigma_v)^2 + (\alpha\sigma_2)^2 + 4g^2\sigma_v\sigma_2}}{2}$$

Since σ_v and σ_2 are very small,

$$-1 \ll s_{2,3} < 0, \qquad \forall t \geq 0$$

The rate of decay for $\tilde{x}_2$ and $\tilde{x}_3$ is small and the eigenvector associated with s_2 is around $w_2 \approx [0 \;\; 1 \;\; 1]^T$. Moreover, the eigenvector w_2 is independent of state variables, as shown in Fig. 3. In section 3 we proved that $\tilde{\mathbf{x}} \to \mathbf{0}$ and, from the analysis in this section, we found that the convergence of states $\hat{x}_2$ and $\hat{x}_3$ is very slow, which is illustrated by the numerical example of the previous section. Fig. 3 shows a sketch of the trajectory portrait of the approximate nonlinear system (20). For any initial condition $P_0 = (\tilde{x}_1(0), \tilde{x}_2(0), \tilde{x}_3(0)) \in \mathcal{R}^3$, the flow trajectory will quickly approach to the $\tilde{x}_2 \times \tilde{x}_3$ plane because

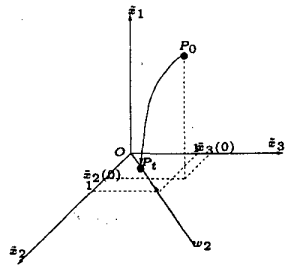

Figure 3: A schematic trajectory plot for nonlinear system $\dot{\tilde{\mathbf{x}}} = \bar{A}(x_3)\tilde{\mathbf{x}}$.

of the rapid convergence of $\tilde{x}_1$ (s_1 is large). Moreover, the trajectory will converge to w_2 on the $\tilde{x}_2 \times \tilde{x}_3$ plane if $\tilde{x}_2(0) > 0$ and $\tilde{x}_3(0) > 0$, as shown in Fig. 3. Thus, if we pick

$$\tilde{x}_2(0) \geq 0, \qquad \tilde{x}_3(0) \geq 0, \tag{21}$$

then

$$\max\{\tilde{x}_2(0), \tilde{x}_3(0)\} \geq \tilde{x}_2(t) \approx \tilde{x}_3(t) \geq 0, \quad \forall t \geq t_0$$

where t_0 is fairly small and depends on the convergence rate and initial conditions of $\tilde{x}_1(t)$.

Remark 4 Note that by Theorem 1 we obtained $\hat{\lambda} \to \hat{\lambda}_{max}$ and $\lambda \to \lambda_{max}$ due to the fact $\hat{\mathbf{x}} \to \mathbf{x}$. However, since the states $\hat{x}_3$ and $\hat{x}_2$ converge slowly, there will be some error between λ and $\hat{\lambda}$. This error can be estimated as follows.

$$\begin{aligned}
\lambda(t) - \hat{\lambda}(t) &= \frac{x_3}{x_2} - \frac{\hat{x}_3}{\hat{x}_2} = \frac{x_2\tilde{x}_3 - x_3\tilde{x}_2}{x_2\hat{x}_2} \\
&\approx \frac{(x_2 - x_3)\tilde{x}_2}{x_2\hat{x}_2} = \left(1 - \frac{x_3}{x_2}\right)\frac{\tilde{x}_2}{\hat{x}_2} \\
&\leq (1 - \lambda(t))\lambda(0), \quad \forall t \geq t_0
\end{aligned}$$

Note that in general $\lambda(0) \leq 3\%$ during normal driving conditions before braking. As a consequence, the slip estimate error is small. Similarly, it can be shown that $\lambda_{max} - \hat{\lambda}_{max}$ will also be small after the state $\tilde{x}_1 \to 0$. Therefore, the proposed control system will achieve a near maximum deceleration level, in spite of the fact that state estimation errors $\tilde{x}_2$ and $\tilde{x}_3$ converge slowly.

6 Conclusions

In this paper we discussed emergency braking control under unknown tire/road conditions and system states, based on a dynamical friction model and the assumption that the only available measurable signal to the controller is the wheel angular velocity. The braking pressure controller is determined based on the estimation of system state variables and the unknown friction parameter. The simulation results show that the vehicle can be stopped quickly with near maximum deceleration by applying this controller. The asymptotic convergence of the estimated states and parameters estimates has been proven. Moreover, it was also shown that the friction properties can be estimated and near maximum deceleration achieved, in spite of the slow convergence rate of the vehicle velocity and wheel relative velocity error estimates. Fortunately, both automated highway systems (AHS) and manual traffic applications rely on various other measurements to guarantee safety; (e.g. radar sensors and human perception). Thus, the control system does not need an accurate estimate of the vehicle velocity. Simulation tests conducted so far suggest that the proposed control scheme, based on an observed dynamic friction model, achieves near maximum deceleration in a faster and more stable manner than previous static approaches. An alternate design, using both the vehicle's linear acceleration with an accelerometer and wheel angular acceleration as in [2] is in progress.

References

[1] L. Alvarez, J. Yi, R. Horowitz, and L. Olmos.-Adaptive Emergency Control in AHS with Underestimation of Friction Coefficient. In *The American Control Conference*, 2000.

[2] L. Alvarez, J. Yi, R. Horowitz, and L. Olmos. Observer-based Emergency Braking Control in Automated Highway Systems. Washington, DC, 2001. To be presented in American Control Conference.

[3] E. Bakker, L. Nyborg, and H.B. Pacejka. Tyre Modelling for Use in Vehicle Dynamic Studies. Society of Automotive Engineers Paper # 870421, 1987.

[4] Carlos Canudas de Wit and Roberto Horowitz. Observers for Tire/Road Contact Friction using only wheel angular velocity information. In *Proceedings of* 38th *IEEE Conference of Decision and Control*, Phoenix, AZ, 1999.

[5] Carlos Canudas de Wit, H. Olsson, K.J. Åström, and P. Lischinsky. A New Model for Control of Systems with Friction. *IEEE Trans. on Automatic Control*, 40(3):419–425, 1995.

[6] Carlos Canudas de Wit and Panagiotis Tsiotras. Dynamic Tire Friction Models for Vehicle Traction Control. In *Proceedings of* 38th *IEEE Conference of Decision and Control*, Phoenix, AZ, 1999.

[7] Young Man Cho and Rajesh Rajamani. A Systematic Approach to Adaptive Observer Synthesis for Nonlinear Systems. *IEEE Transactions on Automatic Control*, 42(4):534–537, 1997.

[8] L. El Ghaoui, R. Nikoukhah, and F. Delebecque. LMITOOL: a Package for LMI Optimization. In *Proceedings of* 34th *IEEE Conference of Decision and Control*, 1999.

[9] U. Kiencke. Realtime Estimation of Adhesion Characteristic Between Tyres and Road. In *Proceedings of the IFAC World Congress*, volume 1, 1993.

[10] J. Y. Wong. *Theory of Ground Vehicles.* John Wiley & Sons, New York, NY, 2nd edition, 1993.

[11] J. Yi, L. Alvarez, R. Horowitz, and C. Canudas de Wit. Adaptive Emergency Braking Control in Automated Highay System Using a Dynamic Tire/road Friction Model. In *Proceedings of* 39th *IEEE Conference of Decision and Control*, 2000.